Electronic Supplementary Material (ESI) for RSC Advances.

High and Selective Sorption of C_2 Hydrocarbons in Heterometal-Organic Frameworks Built from Tetrahedral Units

Yan-Xi Tan, Yan-Ping He and Jian Zhang*

State Key Laboratory of Structural Chemistry, Fujian Institute of Research on the Structure of Matter, Chinese Academy of Sciences, Fuzhou, Fujian 350002, P. R. China. E-mail: zhj@fjirsm.ac.cn

Experimental Section

General Procedures. All reagents were purchased commercially and used without further purification. All Powder X-ray diffraction (PXRD) analyses were recorded on a Rigaku Dmax2500 diffractometer with Cu Kα radiation (λ = 1.54056 Å) with a step size of 0.05°. Thermal stability studies were carried out on a NETSCHZ STA-449C thermoanalyzer with a heating rate of 10 °C/min under an N_2 atmosphere. Gas adsorption measurement was performed in the ASAP (Accelerated Surface Area and Porosimetry) 2020 System. Nonlinear optical (NLO) properties were measured by Kurtz−Perry powder SHG test using an Nd:YAG laser (1064 nm) with an input pulse of 350 mV.

Synthesis of $[AgIn(na)_4]\cdot 1.5DMF$ (1): Hna (246 mg, 2 mmol), $AgNO_3$ (85 mg, 0.5 mmol) and $In(NO_3)_3$ (150 mg, 0.5 mmol) were dissolved in 8 mL DMF, which were placed in a 20 mL vial. The mixture was heated at 100 °C for 12 hours, and then cooled to room temperature. Colorless block crystals of the product were formed and collected by filtration and washed with DMF several times (Yield: 220 mg, 55%, based on Hna).

Synthesis of $[CuIn(na)_4]\cdot 1.5DMF$ (2): The procedure was the same as that for **2** except that $AgNO_3$ was replaced by CuI. Yellow block crystals of **2** were obtained in 10% yield based on Hna.

X-ray Crystallographic Study: The diffraction data for compounds were collected on an Oxford Xcalibur diffractometer equipped with a graphite–monochromatized Mo-Kα radiation (λ = 0.71073 Å) at 293(2) K. Crystal data for 1: $C_{24}H_{16}N_4O_8AgIn$, M = 711.10, orthorhombic, a = 10.8851(12) Å, b = 11.8615(10) Å, c = 13.9326(10) Å, β = 90.000°, V = 1798.9(3) Å^3, T =

293(2) K, space group *I222*, Z = 2, 2661 reflections measured, 1923 independent reflections (R_{int} = 0.0600). The final R_1 value was 0.0612 ($I > 2\sigma(I)$). The final $wR(F^2)$ value was 0.1564 ($I > 2\sigma(I)$). The goodness of fit on F^2 was 1.053. Crystal data for 2: $C_{24}H_{16}N_4O_8CuIn$, M = 666.78, monoclinic, a = 11.1032(6) Å, b = 11.1032(6) Å, c = 13.8084(9) Å, β = 90.000°, V = 1702.31(17) Å ^{3}, T = 293(2) K, space group *I-42m*, Z = 2, 2031 reflections measured, 957 independent reflections (R_{int} = 0.0432). The final R_1 value was 0.0391 ($I > 2\sigma(I)$). The final $wR(F^2)$ value was 0.1207 ($I > 2\sigma(I)$). The goodness of fit on F^2 was 1.199. The structures were solved by the direct method and refined by the full-matrix least-squares on F^2 using the SHELXTL–97 program. The SQUEEZE routine of the PLATON software suite was used to remove the highly disordered solvent molecules of compounds **1** and **2**.

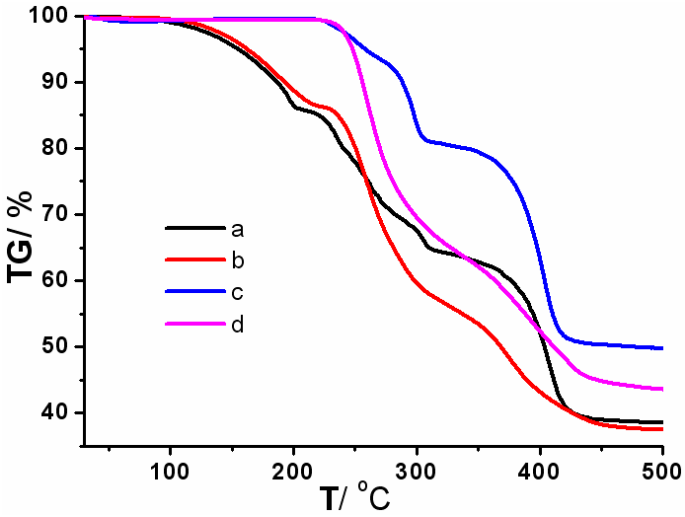

Figure S1. TGA curves of **1** (a), **2** (b), **1a** (a) and **2a** (b).

The TGA of **1** was performed under N_2 atmosphere with a heating rate of 10 °C/min in the temperature range 30–500 °C. As shown in Figure S1a, **1** shows a weight loss of 13.8 % in the temperature range of 225–440 °C, corresponding to the release of 1.5 DMF molecules per unit cell. Further weight loss of 47.1% is observed at ca. 440 °C, owing to the decomposition of the ina ligands. Finally, the residue of 38.7% may be the In_2O_3 and Ag_2O powder. The similar weight losses can be seen in the TGA curves of **2**. The TGA curves of **1a** and **2a** indicate the complete withdraw of guest after heating CH_2Cl_2-exchanged **1** and **2** under high vacuum at 60 ^oC for 24 hours.

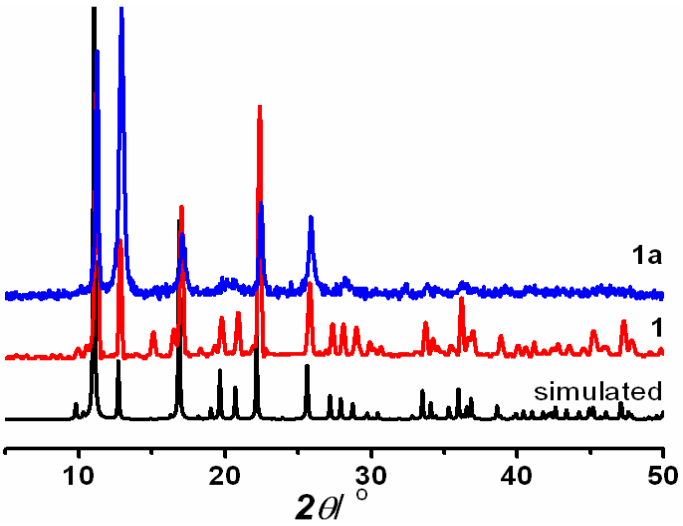

Figure S2. The PXRD patterns of simulated one (a), **1** and **1a**

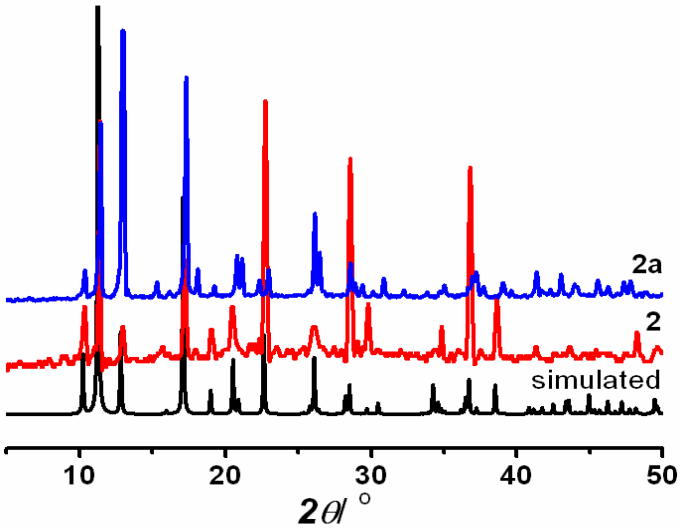

Figure S3. The PXRD patterns of simulated one (a), **2** and **2a**

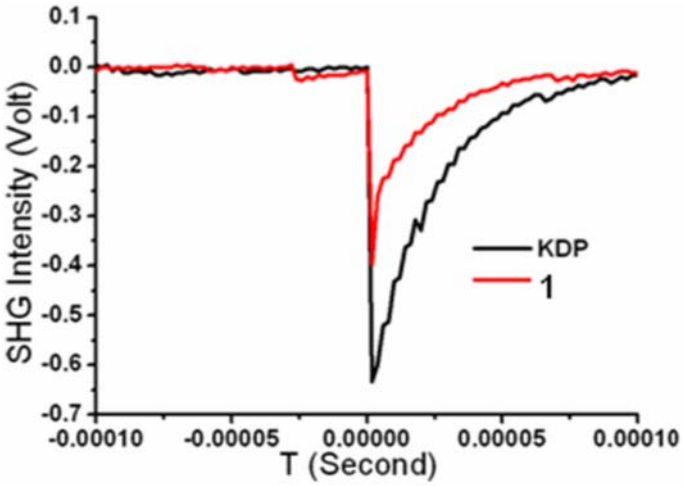

Figure S4. Comparison of the measured SHG response of **1** with that of KDP

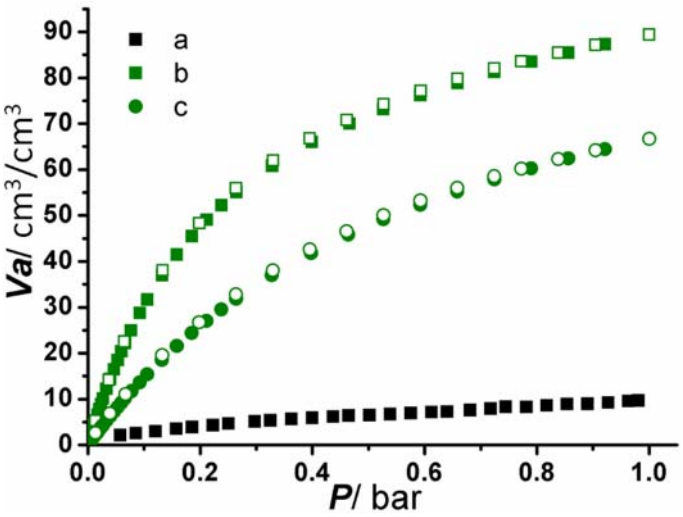

Figure S5. Gas sorption isotherms for **2a**: N_2 at 77 K (a), CO_2 at 273 K (b) and 298 K (c).

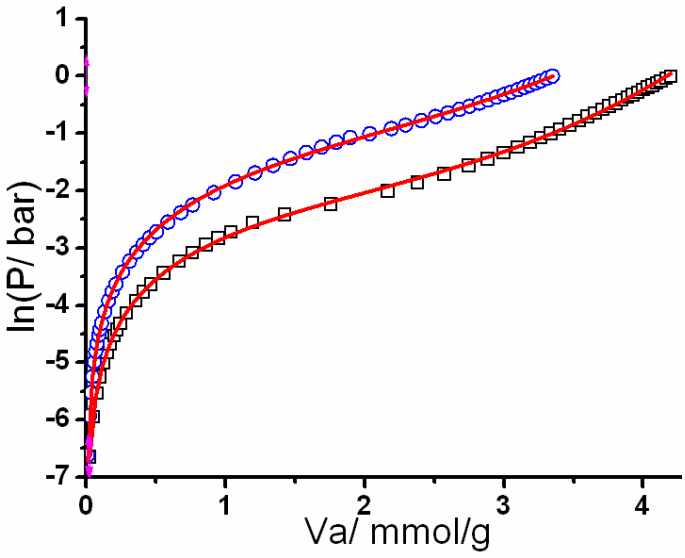

Figure S6. CO_2 adsorption isotherms for **1a** fitting by virial method.

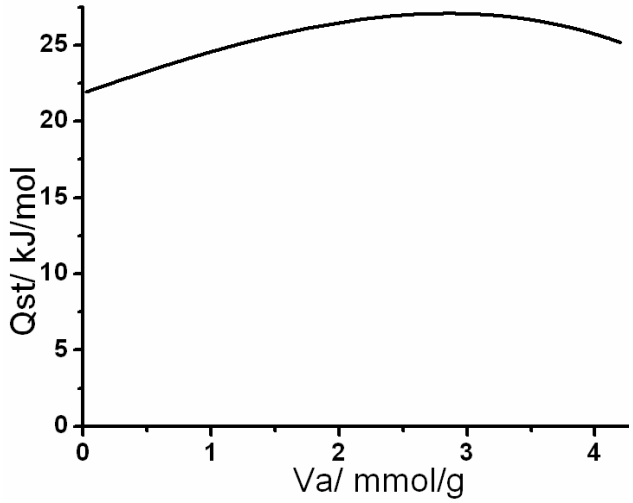

Figure S7. The isosteric heat of CO_2 adsorption for **1a** estimated by the virial equation.

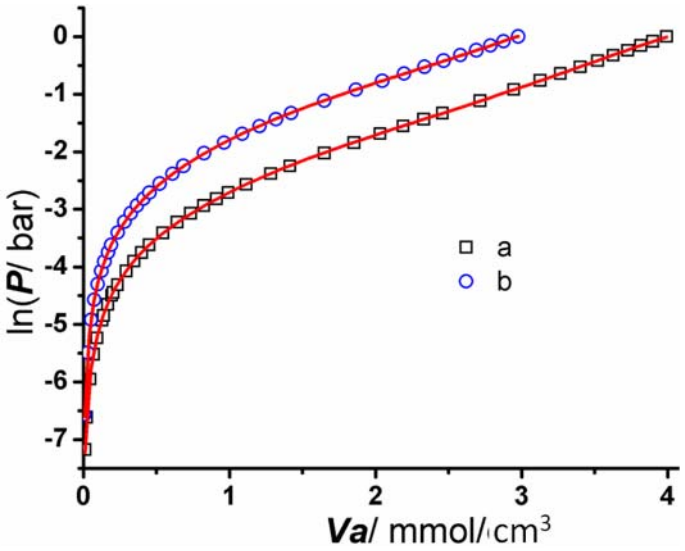

Figure S8. CO_2 adsorption isotherms for **2a** fitting by virial method.

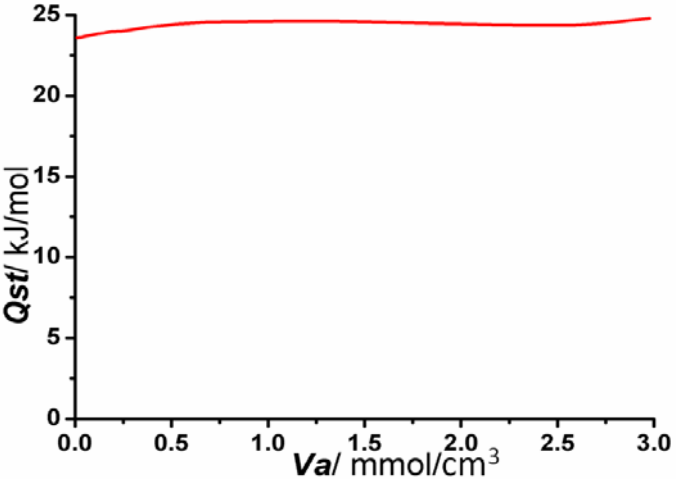

Figure S9. The isosteric heat of CO_2 adsorption for **2a** estimated by the virial equation.

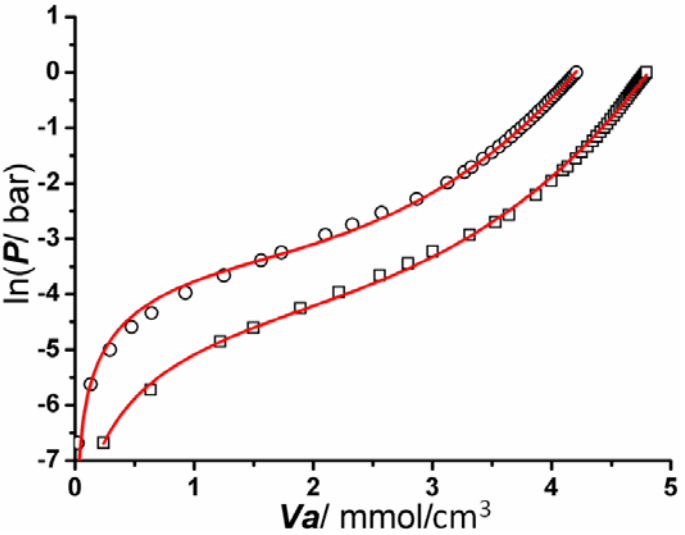

Figure S10. C_2H_6 adsorption isotherms for **1a** fitting by virial method.

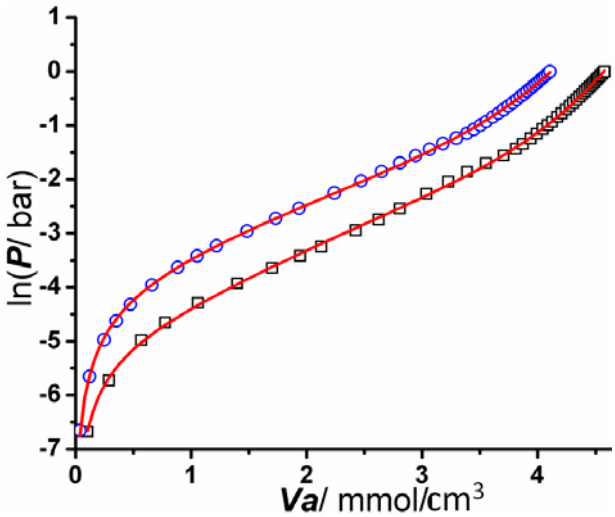

Figure S11. C_2H_4 adsorption isotherms for **1a** fitting by virial method.

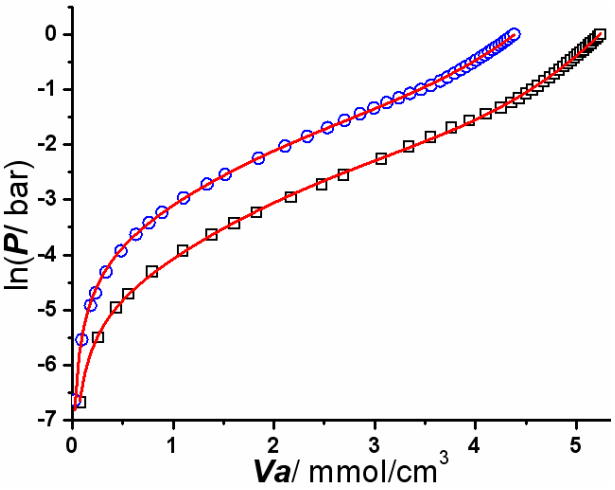

Figure S12. C_2H_2 adsorption isotherms for **1a** fitting by virial method.

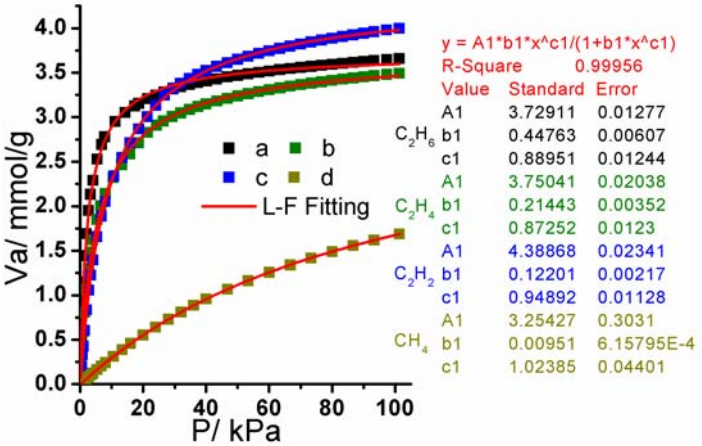

Figure S13. Adsorption isotherms for C_2H_6 (a), C_2H_4 (b), C_2H_2 (c) and CH_4 (d) in **1a** at 273 K. Solid lines through the experimental data are fits to the dual-site Langmuir-Freundlich model.